

Full Length Research Paper

Interface energy of solid cadmium (Cd) phase in the Cd-Pb (Cadmium-Lead) binary alloy

Fatma Meydaneri^{1*}, Buket Saatçi² and Ahmet Ülgen³

¹Department of Metallurgy and Materials Engineering, Faculty of Engineering, Karabük University, 78050, Karabük, Turkey.

²Department of Physics, Faculty of Arts and Sciences, Erciyes University, 38039, Kayseri, Turkey.

³Department of Chemistry, Faculty of Arts and Sciences, Erciyes University, 38039, Kayseri, Turkey.

Accepted 14 February, 2013

The grain boundary groove shapes for the Cadmium (Cd) phase in equilibrium with the Lead (Pb)-Cd eutectic liquid were obtained with radial heat flow apparatus. From the obtained grain boundary groove shapes, the Gibbs-Thomson coefficient, solid-liquid and grain boundary energy for the Cd phase in equilibrium with the Pb-Cd eutectic liquid were determined to be $(8.35 \pm 0.41) \times 10^{-8}$ Km, $(128.00 \pm 12.8) \times 10^{-3}$ Jm⁻² and $(239.33 \pm 26.32) \times 10^{-3}$ Jm⁻², respectively. The thermal conductivities of the solid and liquid phases at the eutectic composition and temperature were also measured by using radial heat flow and Bridgman-type directional growth apparatus, respectively.

Key words: Crystal growth, phase equilibria, thermal conductivity, Gibbs-Thomson coefficient, grain boundary energy.

INTRODUCTION

Despite being hazardous substances cadmium (Cd), Lead (Pb) and their alloys are sometimes used technologically. Cd is a Group IIB element, while Pb is in group IVB of the periodic table. Cd is extensively used in the electroplating and battery industries. Pb is of significant relevance in making cable covering, plumbing, ammunition and as a sound absorber. Eutectic alloys are the basis of most engineering materials, and have relatively low melting points, excellent fluidity, and good mechanical properties. Knowledge of the thermodynamics of materials provides fundamental information about the stability of phases and about the driving forces for chemical reactions and diffusion processes.

Hence, the purpose of this study is to determine some thermodynamic properties such as thermal conductivity coefficients (κ_S , κ_L), Gibbs-Thomson coefficient (I), solid-liquid interfacial energy (σ_{SL}) and the grain boundary

energy (σ_{GB}) of Cd solution in equilibrium with the Pb-Cd eutectic liquid from the observed grain boundary groove shapes. These data are of great importance for the development of electronic, semi-conductor, superconductor materials and interconnection technologies, especially in microelectronics. The solid-liquid surface energy (σ_{SL}) is defined as the reversible work required to create a unit area of the interface at constant temperature, volume and chemical potentials (Woodruff, 1973) and it plays a critical role in phase transformations. Theoretical and experimental works have been made to determine the values of σ_{SL} in various materials by using different methods for the last 50 years. Unfortunately, it is not easy to measure σ_{SL} even for a pure material, and very little progress has been made in its measurement for a multi-component system. One of the most common techniques to determine the solid-liquid interface energy is to use the equilibrated grain boundary groove shapes. Observation of grain boundary groove shape in an alloy is obviously very difficult. The technique was used to measure σ_{SL} of

*Corresponding authors. E-mail: meydaneri@yahoo.com.
Tel:+90 (370) 433 20 21. Fax: +90 (370) 433 20 05.

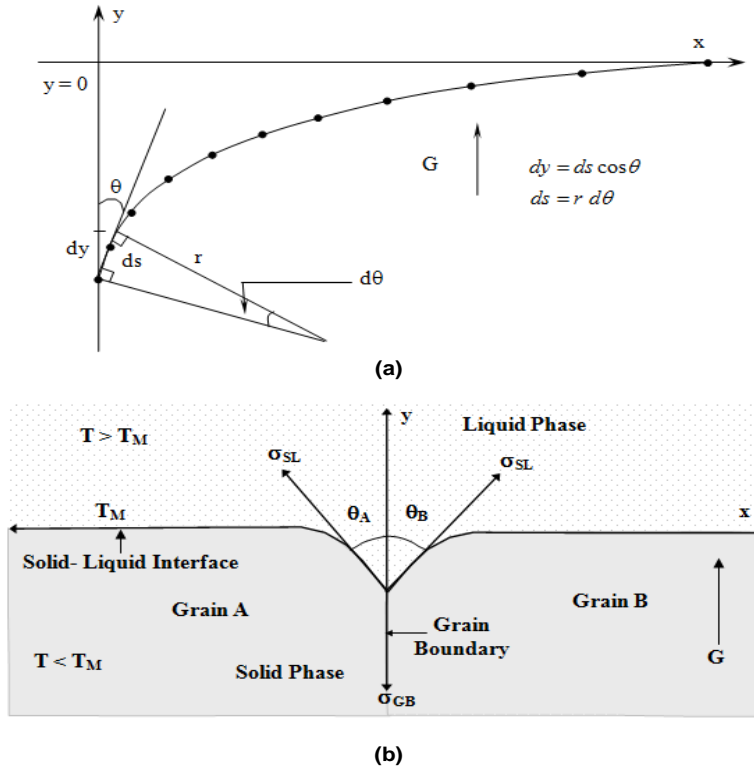


Figure 1. (a) Solid-liquid interface in a temperature gradient, showing the x, y coordinates, σ_{SL} , surface tension, σ_{GB} , grain boundary tension and θ . (b) Schematic illustration of an equilibrated grain boundary groove.

metallic alloy systems by Gündüz and Hunt, and to equilibrium solid-liquid and solid-solid interface in constant temperature gradient (G). Also, Gündüz and Hunt developed a numeric model to calculate the Gibbs-Thomson coefficient (Γ) that the distinguishing characteristics of the materials.

The Gibbs-Thomson coefficient (Γ) is expressed in the form of a change in undercooling ΔT_r with r the radius of the curvature as:

$$\Delta T_r = \frac{\Gamma}{r} \quad (1)$$

Equation 1 can be integrated in the y-direction (perpendicular to the interface in 2D) from the flat interface to a point on the curve

$$\int_0^y \Delta T_r dy = \Gamma \int_0^y \frac{1}{r} dy \quad (2)$$

The left hand side of Equation 2 may be evaluated if ΔT_r is known for any y-point. The thermal conductivities of the solid (κ_S) and liquid (κ_L) phases are not equal so that the left hand side of Equation 2 can be integrated by

using the numerically calculated ΔT_r values (Gündüz and Hunt, 1985, 1989). The right hand side of Equation 2 may be evaluated for any shape by defining $ds = r d\theta$ (s is the distance along the interface and θ is the angle of a tangent to the interface with y-axis (as shown in Figure 1), which is obtained by fitting a Taylor expansion to the adjacent points on the curve) giving

$$\Gamma \int_0^y \frac{1}{r} dy = \Gamma (1 - \sin \theta) \quad (3)$$

This allows the Gibbs-Thomson coefficient to be determined for a measured grain boundary groove shape. To obtain accurate values of the Gibbs-Thomson coefficient the shape of the interface, the temperature gradient in the solid (G_s) and the conductivities of the solid (κ_S) and liquid (κ_L) must be known.

The solid-liquid surface energy is obtained from the thermodynamic definition of the Gibbs-Thomson coefficient which is expressed as:

$$\Gamma = \frac{\sigma_{SL}}{\Delta S^*} \quad (4)$$

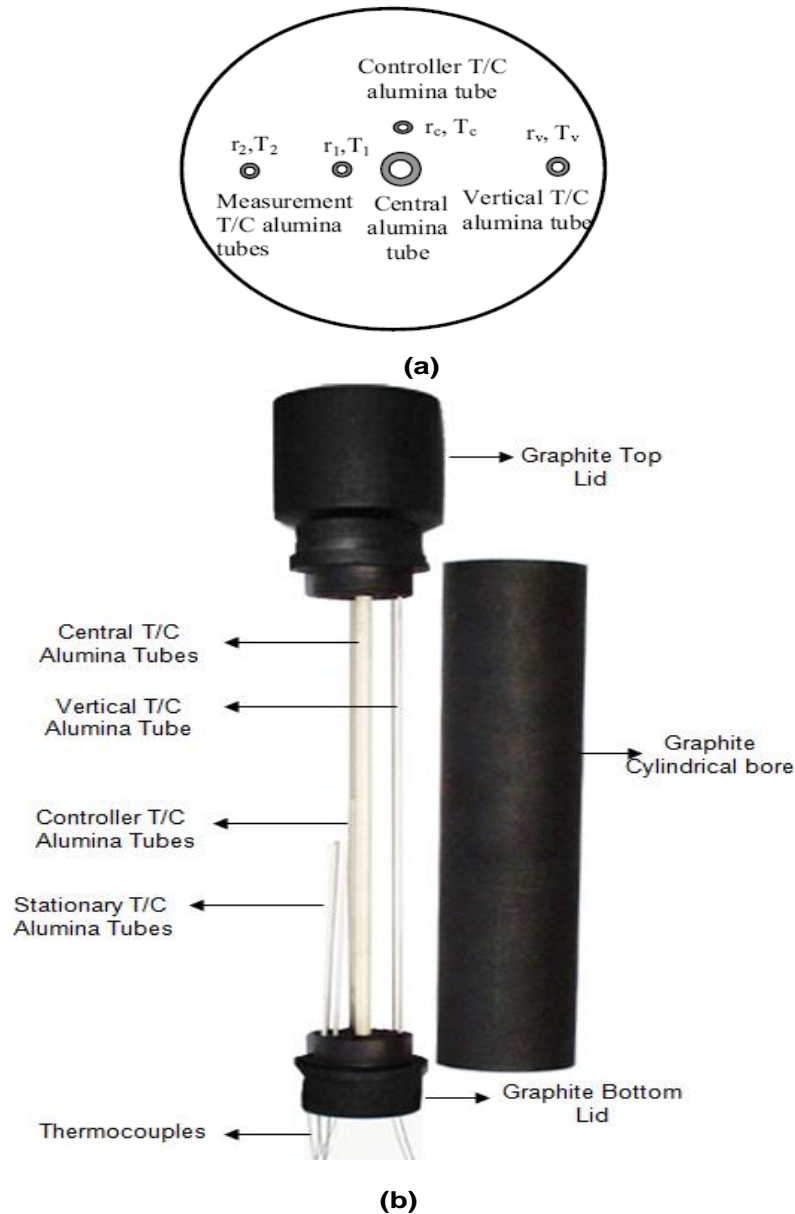


Figure 2. (a) Transverse cross-section of specimen. (b) Longitudinal section of alumina tubes and thermocouples placed to graphite crucible.

where ΔS^* is the effective entropy of melting per unit volume which must be known.

EXPERIMENTAL PROCEDURE

The sample crucible

The sample crucible is composed of three parts, a cylindrical bore (30 mm inner diameter (ID), 40 mm outer diameter (OD) and 170 mm in length), and the top and bottom lids which were tightly fitted to the cylindrical part, as shown in Figure 2. Three stationary thermocouples (inserted in a 0.8 mm ID, 1.2 mm OD alumina tube) were fitted on the bottom lid, while two thermocouples (r_1 and r_2)

were placed 1.0 to 1.5 mm away from the central alumina tube, the other one (r_2) was placed about 11 mm away from the central alumina tube. r_c was used for the control unit, and the other two ($r_2 > r_1$) were used for measuring the temperature. A moveable thermocouple (inserted in a 1 mm ID, 2 mm OD alumina tube) was also placed 10 mm away from the center and used for measuring the vertical temperature variation. Also, a thin-walled central alumina tube (2 mm ID, 3 mm OD) was used to isolate the central heating wire (Kanthal A1) on the bottom lid.

Sample preparation

The phase diagram of Pb-Cd alloy has been examined (Hansen and Anderko, 1985). The composition was determined to be

Cd-20 wt.% Pb to obtain the Cd phase in equilibrium with the eutectic liquid (Cd-17.4 wt.% Pb). (Cd-20 wt.% Pb) alloy was melted in a vacuum furnace by using 4N pure Cd and 4N pure Pb. After several stirrings, the melted alloy was poured into a graphite sample crucible held in a specially constructed casting furnace at approximately 30K above the eutectic temperature, T_E , of the alloy (521K). The molten metal was then directionally solidified from bottom to top to ensure that the sample crucible was completely full. The sample was prepared to be placed in the radial heat flow apparatus.

Radial heat flow apparatus

In order to observe the equilibrated grain boundary groove shapes in eutectic alloy systems, Gündüz and Hunt (1985, 1989) designed a radial heat flow apparatus. Maraşlı and Hunt (1996) improved the experimental apparatus for higher temperature. Recently, Maraşlı and others studied ternary alloy systems by using the apparatus (Akbulut et al., 2009; Ocak et al., 2010; Aksöz et al., 2011). The details of the apparatus and experimental procedures are given in Maraşlı and Hunt (1996), Akbulut et al. (2009), Ocak et al. (2010), Aksöz et al. (2011), Meydaneri et al. (2011, 2012), Saatçi et al. (2007), and Bulla et al. (2007). In the present work, a similar apparatus was used to observe the grain boundary groove shapes of the solid (Cd - 0.25 wt.% Pb) solution in equilibrium with the (Cd-17.4 wt.% Pb) eutectic liquid. A schematic illustration of the radial heat flow apparatus and the block diagram of the experimental system are shown in Figure 3.

Equilibration of the sample

The central heating wire (Kanthal A1, typically about 1.7 mm diameter and 200 mm in length) was placed inside a thin-walled central alumina tube. The terminal-points of the heating element were threaded and screwed into 7 mm copper rods. The casting sample was placed inside a water cooled jacket, and to increase the experimental sensitivity, the gap between the cooling jacket and the specimen was filled with free running sand. Then, the thermocouples (K type, 0.5 mm thick insulated) were placed into alumina tubes fixed on the bottom lid, and the jacket was placed in the radial heat flow apparatus. The sample was heated from the center by the heating wire and the outside of the sample was kept cool with the water cooling jacket. A thin layer (1 to 3 mm thick) was melted around the central heating wire and the specimen was annealed in a very stable temperature gradient for 18 days to get the equilibrium solid solution (Cd-0.25 wt.% Pb) with the eutectic liquid (Cd-17.4 wt.% Pb). The temperature on the sample was controlled to an accuracy of ± 0.01 K with a *Eurotherm 9706* type controller. The temperature control was procured by measuring the oscillation period (PID) and setting actual time constants. During the annealing period, the temperature in the specimen and the longitudinal temperature variations on the sample were continually recorded by the stationary thermocouples and a moveable thermocouple, respectively, by using a *Pico TC-08* data-logger via computer. The potential difference (V_h) between the ends of the central heating element was measured with Hewlett Packard 34401 multimeters. The current (I) passing from the central heating wire was measured with a TES 3012 Digital Clampmeter. The input power was also recorded periodically. The temperature in the sample was stable at about ± 0.01 to 0.02 K for hours and ± 0.05 K for up to 18 days. Effective cooling is very important to obtain a high temperature gradient and a well quenched solid-liquid interface. At the end of the annealing time the specimen was rapidly quenched by turning off the input power.

Metallography

The equilibrated sample was removed from the furnace and cut transversely into ~ 20 mm lengths. The transverse sections were ground flat with 800, 1000, and 2400 grid SiC papers, respectively, before mounting. Grinding and polishing were then carried out using the standard techniques. After polishing, the samples were etched with a suitable etchant (5 ml nitric acid + 5 ml acetic acid + 90 ml glycerin) to observe the equilibrated solid-liquid interface.

The equilibrated grain boundary groove shapes which occurred on the solid-liquid interface were carefully photographed with a charge couple device (CCD) digital camera placed on top of an *Olympus BH2* light optical microscope using a 40 x objective. A graticule ($100 \times 0.01 = 1$ mm) was also photographed using the same objective. The digital camera had rectangular pixels. Thus, the magnifications in the x and y directions are different. The photographs of the equilibrated grain boundary groove shapes and the graticule in the x and y directions were photographed by using *Adobe Photoshop CS2* version software, so that accurate measurements of the groove coordinate points on the groove shapes could be made.

Geometrical correction for the groove coordinates

In order to obtain accurate Γ values by the numerical method, not only the G and κ_S , values but also the coordinates on the grain boundary grooves must be measured accurately. The coordinates of the cusp, x, y should be measured using the coordinates x' , y' , z where the x-axis is parallel to the solid-liquid interface, the y axis is normal to the solid-liquid interface and the z axis lies at the base of the grain boundary groove as shown in Figure 4a. The coordinates of the cusp x' , y' from the metallographic section must be transformed to the x, y coordinates. Maraşlı and Hunt devised a geometrical method to make appropriate corrections to the groove shapes and the details of the geometrical method are given in Maraşlı and Hunt (1996). The relation between x and x' can be expressed as:

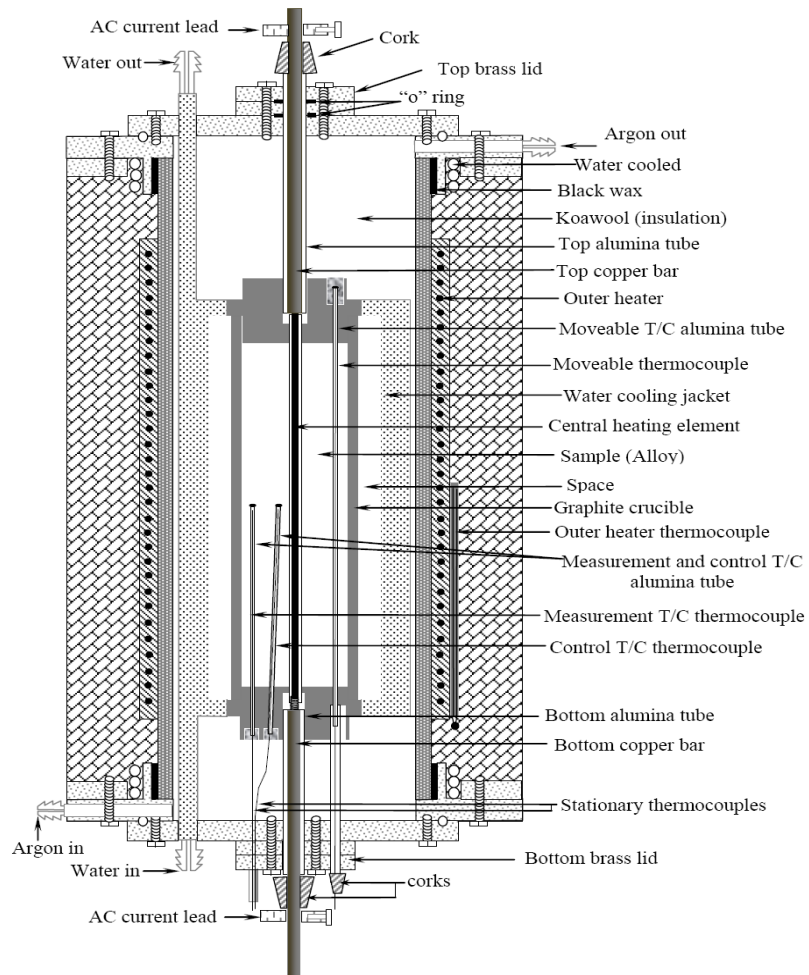
$$x = x' \cos \alpha = x' \frac{\sqrt{a^2 + d^2}}{\sqrt{a^2 + b^2 + d^2}} \quad (5)$$

and the relation between y' and y can be expressed as:

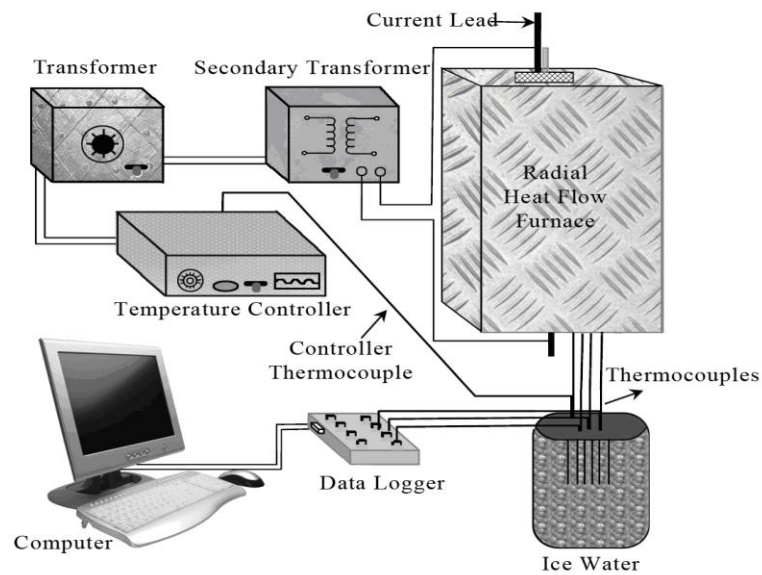
$$y = y' \cos \beta = y' \frac{d}{\sqrt{a^2 + d^2}} \quad (6)$$

where d is the distance between the first and second plane along the z' axis, b is the displacement of the grain boundary position along the x' axis, a is the displacement of the solid-liquid interface along the y' axis, α is the angle between the x' axis and x axis, and β is the angle between the y' axis and y axis as shown in Figure 4. In this work, the values of a , b and d were measured in order to transform the cusp coordinates x' , y' into the x, y coordinates as follows.

Two perpendicular reference lines (approximately 0.1 mm thick and 0.1 mm deep) were marked near the grain boundary groove on the polished surface of the sample as shown in Figure 4c. The samples were then polished and the grain boundary groove shapes were photographed. The thickness of the sample d_1 was measured with a digital micrometer (resolution of 1 μ m) at several points of the sample to obtain the average value. After the thickness measurements had been made the sample was again polished to remove a thin layer (approximately 40 to 50 μ m) from the sample surface. The same grain boundary groove shapes were again photographed and the thickness of the sample d_2 was measured



(a)



(b)

Figure 3. (a) Schematic illustration of radial heat flow apparatus. (b) The block diagram of the experimental system.

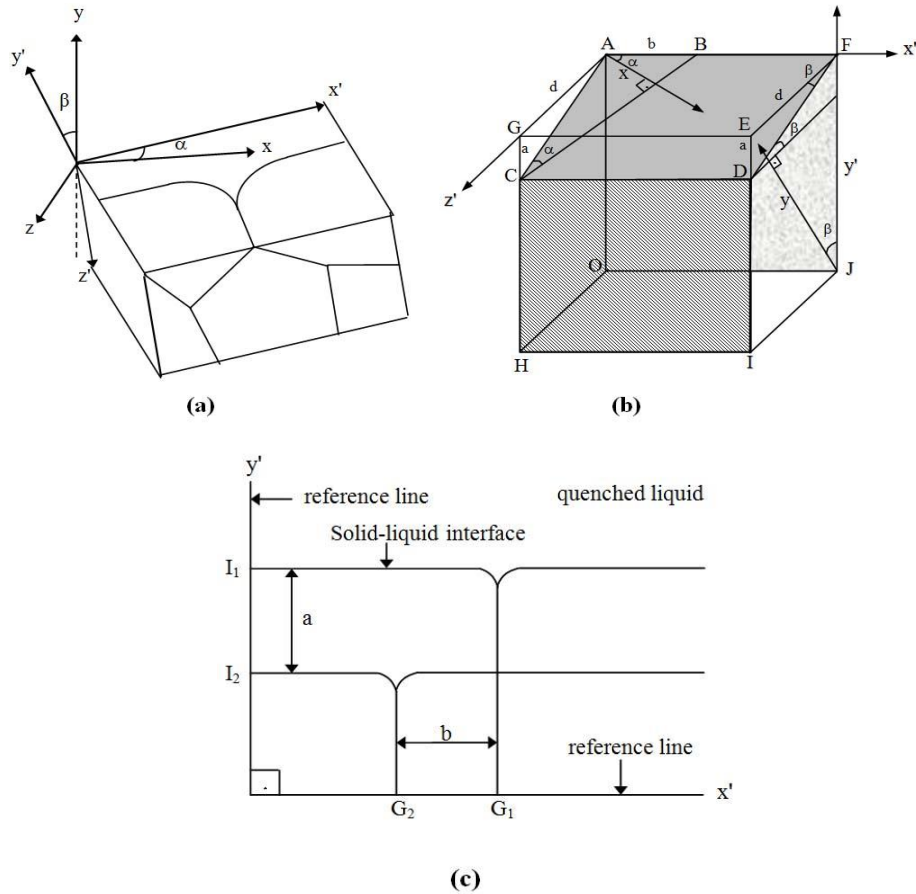


Figure 4. (a) Schematic illustration of the relationship between the actual coordinates, x , y and the measured coordinates, x' , y' of the groove shape. (b) Schematic illustration for the metallic examination of the sample: where B is the location of the grain boundary groove shape onto first plane OJFA, C is the location of the grain boundary groove shape onto second plane HJDC, $AB = b$, $CG = ED = a$ and $AG = d$. (c) Schematic illustration of the displacement of the grain boundary groove shape position along the x' and y' axis (Maraşlı and Hunt, 1996).

with the same micrometer. The difference between the thickness of the sample, $d = d_1 - d_2$, gave the layer removed from the sample surface. The photographs of the grain boundary groove shapes were mounted on one another using *Adobe Photoshop CS2* version software to measure the displacement of the solid-liquid interface along the y' axis and the displacement of the grain boundary groove position along the x' axis (Figure 4b).

Thus, the required a , b and d measurements were made so that appropriate corrections to the shape of the grooves could be deduced. As shown in Equations 5 and 6, if the values of a , b and d are measured, then the groove coordinates, x' , y' can be transformed into x , y coordinates.

The thermal conductivity of the solid and liquid phases

The radial heat flow method is the most appropriate technique for measuring the conductivities in the solid phase. The thermal conductivity of the solid Cd solution is also needed to calculate the temperature gradient on the solid phases. The sample crucible was made from graphite to measure the thermal conductivity of the sample, as shown in Figure 2.

The sample was heated up in steps of 50K up to 513K (8K below T_E). First, isotherms macroscopically parallel to the axial center of the sample were obtained for the expected temperature, by moving the central heater wire up and down, and the sample was kept at this steady state condition for about 2 h. Then the total input power Q and T_1 , T_2 temperatures were recorded with a *Hewlett Packard 34401* type multimeter, *TES 3012 Digital Clampmeter* and a *Pico TC-08* data-logger at this condition. Finally, the sample was left to cool to room temperature. The cooled sample was moved from the radial heat flow apparatus and was cut transversely near to the measurement points.

The transversely cut samples were ground and polished for r_1 and r_2 measurements. The distances were measured with an *Olympus BH2* light optical microscope to an accuracy of ± 0.01 mm. The transverse and longitudinal sections of the sample were examined for porosity, cracks and casting defects to make sure that these would not introduce any errors to the measurements. The temperature gradient in the cylindrical specimen is given by Fourier's law

$$G_s = \left(\frac{dT}{dr} \right) = - \frac{Q}{A\kappa_s} \tag{7}$$

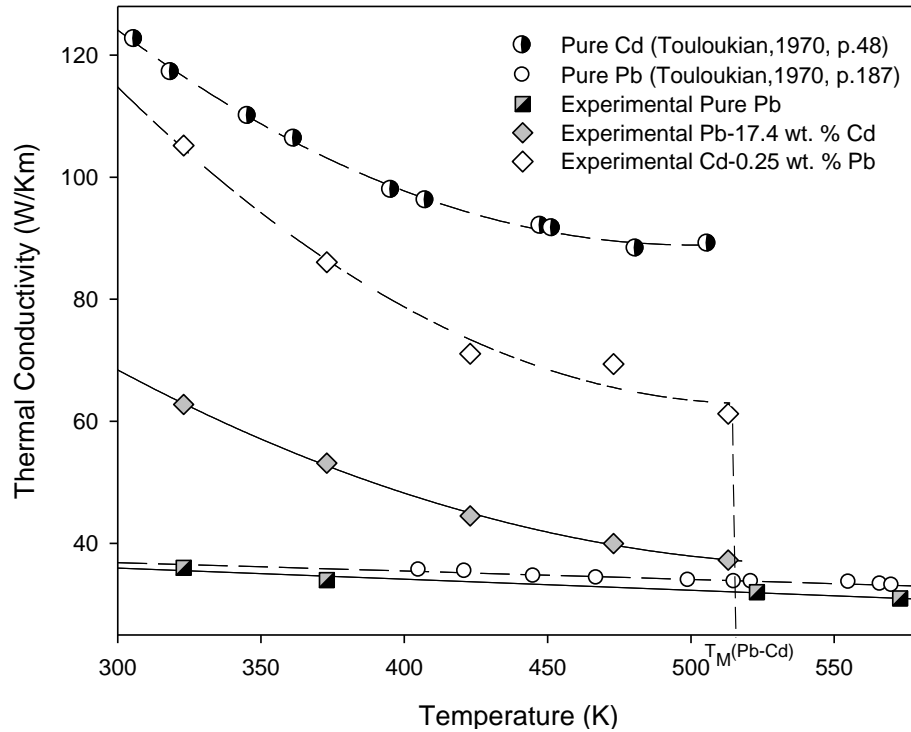


Figure 5. Thermal conductivities of solid phases versus temperature for pure Cd (Touloukian et al., 1970, p.48), pure Pb (Touloukian et al., 1970, p. 187), experimental pure Pb, experimental Cd-17.4 wt.% Pb and experimental Cd-0.25 wt.% Pb alloys.

where Q is the total input power from the center of the specimen, A is the surface area of the specimen and κ_S is the thermal conductivity of the solid phase. Integration of Equation 7 gives

$$\kappa_S = \frac{1}{2\pi\ell} \ln\left(\frac{r_2}{r_1}\right) \frac{Q}{(T_1 - T_2)} \quad (8)$$

where ℓ is the length of the heating element, r_1 and r_2 are the fixed distances from the center of the sample, and T_1 and T_2 are the temperatures at the fixed positions ($r_2 > r_1$) r_1 and r_2 , respectively. If Q , r_1 , r_2 , T_1 and T_2 can be accurately measured for a well-characterized sample, then reliable κ_S values can be determined (Erol et al., 2005). The κ_S values at the melting temperatures of the materials were obtained by extrapolating the thermal conductivity curves to the melting temperature. The thermal conductivity values of the eutectic solid solution (Cd-17.4 wt.% Pb) and solid solution (Cd-0.25 wt.% Pb), κ_S , were obtained as 35.94 and 62.60 W/Km, respectively. The thermal conductivity variation of the solid phases for the materials with temperature is shown in Figure 5. The thermal conductivity ratio of the equilibrated eutectic liquid phase (Cd-17.4 wt.% Pb) to the solid solution (Cd-0.25 wt.% Pb), $R = \kappa_L(\text{liquid}(Cd - 17.4 \text{ wt.}\% \text{ Pb solution})) / \kappa_S(\text{solid}(Cd - 0.25 \text{ wt.}\% \text{ Pb}))$ must be calculated to obtain the Gibbs-Thomson coefficients with the numerical method. The thermal conductivity ratio can be obtained by a Bridgman-type growth apparatus. The heat flow away from the interface through the solid phase must balance that of the heat flow through the liquid phase plus the latent heat generated at the interface, that is, (Porter and Easterling, 1991)

$$VL = \kappa_S G_S - \kappa_L G_L \quad (9)$$

where V is the growth rate, L is the latent heat, and G_S and G_L are the temperature gradients in the solid and liquid phases, respectively, and κ_S and κ_L are the thermal conductivities of the solid and liquid phases, respectively. For low growth rates, $VL \ll \kappa_S G_S$, so that the conductivity ratio, R , is given by

$$\kappa_L G_L \cong \kappa_S G_S, \quad R = \frac{\kappa_L}{\kappa_S} = \frac{G_S}{G_L} \quad (10)$$

The directional growth apparatus, first constructed by McCartney (1981), was used to find the thermal conductivity ratio, $R = \kappa_L / \kappa_S$. A thin-walled graphite crucible, 6.3 mm OD \times 4 mm ID \times 180 mm length, was used to minimize convection in the liquid phase. Molten eutectic alloy (Cd-17.4 wt.% Pb) was poured into the thin-walled graphite tube and the molten alloy was then directionally frozen from bottom to top to ensure that the crucible was completely full.

The specimen was then placed in the Bridgman directional growth apparatus. The specimen was heated to 30K over the melting temperature of the alloy. The specimen was then left to reach thermal equilibrium for at least 2 h. The temperature in the specimen was measured with insulated K type thermocouples. In the present work, a 1.2 mm OD \times 0.8 mm ID alumina tube was used to insulate the thermocouple from the molten alloy, and the thermocouples were placed vertical to the heat flow direction. At the end of equilibration, the temperature in the specimen was stable to ± 0.5 K for the short term period and to ± 1 K for the long term period. When the specimen temperature stabilized, the directional growth was begun by turning the motor on. The cooling rate was recorded with a data-logger via computer.

The velocity of the motor used in the present work was

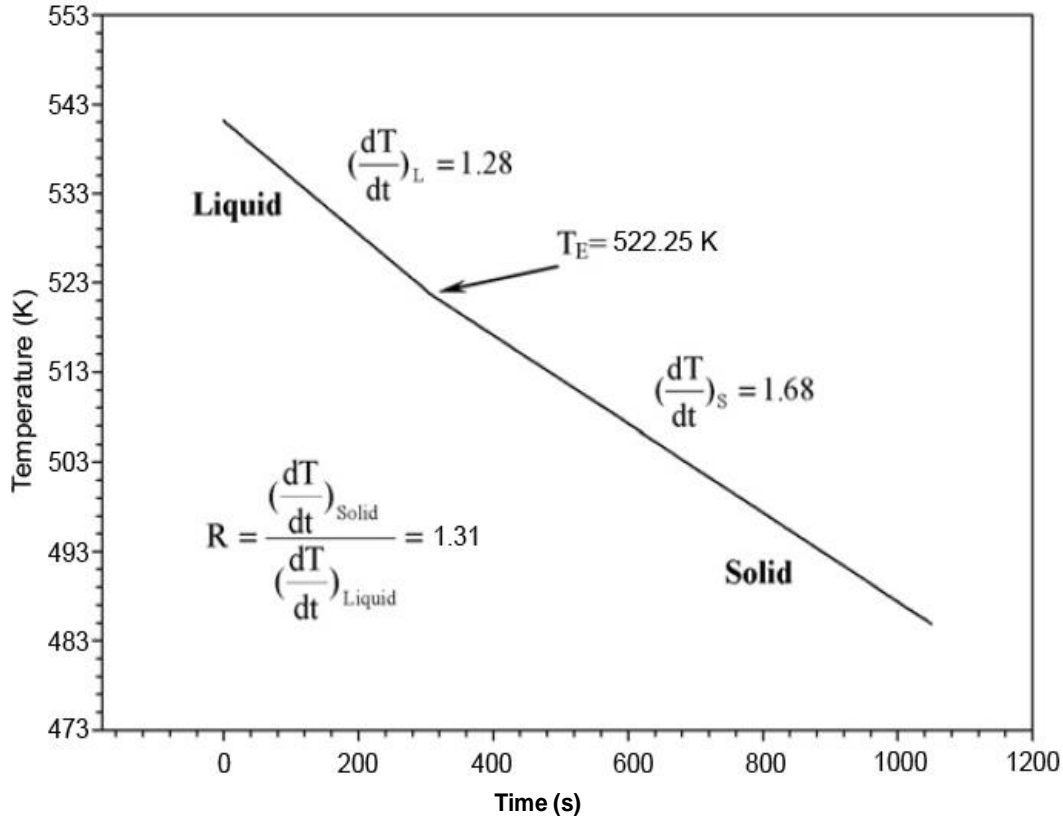


Figure 6. Cooling curve for the eutectic Cd-17.4 wt.% Pb alloy.

5 mm/min, while the solid-liquid interface passed the thermocouples, the slope of the cooling rate for the liquid and solid phases was observed. When the thermocouple reading reached approximately 40 to 50K below that of the melting temperature, the growth was stopped by turning the motor off. The thermal conductivity ratio was obtained from the cooling rate ratio of the liquid phase to the solid phase. The cooling rate of the liquid and solid phases is given by:

$$\left(\frac{dT}{dt}\right)_L = \left(\frac{dT}{dx}\right)_L \left(\frac{dx}{dt}\right)_L = G_L V \quad (11)$$

and

$$\left(\frac{dT}{dt}\right)_S = \left(\frac{dT}{dx}\right)_S \left(\frac{dx}{dt}\right)_S = G_S V \quad (12)$$

From Equations 11 and 12, the thermal conductivity ratio can be written as:

$$R = \frac{\kappa_L}{\kappa_S} = \frac{G_S}{G_L} = \frac{\left(\frac{dT}{dt}\right)_S}{\left(\frac{dT}{dt}\right)_L} \quad (13)$$

where $\left(\frac{dT}{dt}\right)_S$ and $\left(\frac{dT}{dt}\right)_L$ values were directly measured from the temperature versus time, and the cooling curve is shown in Figure 6. The thermal conductivity ratio of the eutectic liquid to the eutectic

solid, $R = \kappa_L(\text{eutectic}) / \kappa_S(\text{eutectic})$ was found to be 1.31.

The thermal conductivity value of the eutectic solid solution (Cd-17.4 wt.% Pb), κ_S , was obtained as 35.94 W/Km. Therefore, the thermal conductivity value of the (Cd-17.4 wt.% Pb) eutectic liquid solution, κ_L , was obtained as 47.08 W/Km. According to the Pb-Cd phase diagram, the solid solubility of Pb in Cd is very restricted and suggested a solubility (about 0.25 wt.%) Pb at the eutectic temperature of 521K. The thermal conductivity of the κ_S (solid Cd-0.25 wt. % Pb) was found to be 62.60 W/Km. The value of $R = \kappa_L(\text{liquid}(Cd - 17.4 \text{ wt. \% Pb solution})) / \kappa_S(\text{solid}(Cd - 0.25 \text{ wt. \% Pb}))$ was found to be 0.76. The values of thermal conductivity used in the calculations are given in Table 1.

Measurement of temperature gradient in the solid phase

At the steady-state the temperature gradient at radius r is given by

$$G_S = \frac{dT}{dr} = -\frac{Q}{2\pi r \ell \kappa_S} \quad (14)$$

where Q is the input power, ℓ is the length of the heating wire, r is the distance to the solid-liquid interface from the center of the sample and κ_S is the thermal conductivity of the solid phase. The average temperature gradient of the solid phase must be determined for each grain boundary groove shape. The temperature gradient of the Cd solid phase was calculated by using the measured values in Equation 14 for each grain boundary groove shape (Table 2).

Table 1. Thermal conductivity of solid and liquid phases in Cd-Pb alloy system.

Alloy	Phase	Melting temperature (K)	κ (W/Km)	$R = \kappa_L/\kappa_S$
Pb-Cd (Eutectic Composition)	(Solid Phase) Cd-17.4 wt.% Pb	521	35.94	1.31
	(Liquid Phase) Cd-17.4 wt. % Pb		47.08	
Pb-Cd	(Solid Phase) Cd-0.25 wt. % Pb	521	62.60	0.76
	(Liquid Phase) Cd-17.4 wt. % Pb		47.08	

Table 2. Gibbs-Thomson coefficients for the solid Cd phase in equilibrium with the eutectic liquid.

Groove No.	α°	β°	$G_S \times 10^2$ (K/m)	Gibbs-Thomson coefficient	
				$\Gamma_{LHS} \times 10^{-8}$ (Km)	$\Gamma_{RHS} \times 10^{-8}$ (Km)
1	17.06	10.87	14.98	8.55	8.69
2	27.07	29.88	16.31	8.51	8.73
3	14.95	6.10	16.08	8.15	8.85
4	17.23	6.05	19.45	8.49	8.64
5	9.17	9.47	17.17	7.56	8.56
6	36.33	23.41	16.19	8.76	8.65
7	9.74	3.68	19.38	8.87	7.21
8	16.42	2.50	19.53	8.11	8.87
9	5.54	11.41	19.28	7.50	7.95
10	5.27	16.94	16.21	8.37	7.99

$\bar{\Gamma} = (8.35 \pm 0.41) \times 10^{-8}$ Km.

RESULTS AND DISCUSSION

The Gibbs-Thomson coefficient

When the thermal conductivity of the solid phase, κ_S , and the thermal conductivity of the liquid phase, κ_L , are not equal, ($\kappa_S \neq \kappa_L$), the curvature under cooling, ΔT_r , is no longer a linear function of the distance. If the thermal conductivity ratio ($R = \kappa_L/\kappa_S$) of the equilibrated liquid phase to solid phase, the coordinates of the grain boundary groove shapes, geometric correction factors and the temperature gradients for each grain boundary groove shape are known, the Gibbs-Thomson coefficients (Γ) can be obtained using the numerical method. The numerical method is described in detail in Gündüz and Hunt (1985, 1989).

In this study, the values of Γ for the solid Cd solution in equilibrium with the eutectic liquid (Cd-17.4 wt.% Pb) were determined by this numerical method using ten equilibrated grain boundary groove shapes, and the results are given in Table 2. Typical grain boundary groove shapes for the solid Cd phase in equilibrium with the eutectic liquid are shown in Figure 7. As can be seen from Figure 7, the grains and interfaces of the system are very clear. The average value of Γ is found to be $(8.35 \pm 0.41) \times 10^{-8}$ km for solid Cd (Table 2).

The effective entropy change

It is also necessary to know the entropy of fusion per unit volume, ΔS^* , for the solid phase to determine the solid-liquid interfacial energy and the entropy change per unit volume for an alloy is given by Gündüz and Hunt (1985):

$$\Delta S^* = \frac{(1 - C_S)(S_A^L - S_A^S) + C_S(S_B^L - S_B^S)}{V_S} \quad (15)$$

where S_A^L , S_A^S , S_B^L and S_B^S are the partial molar entropies for A and B materials and C_S is the solid composition. Since the entropy terms are generally not available, for convenience, the undercooling at constant composition may be explained by the change in composition at constant temperature.

For a spherical solid (Christian, 1975)

$$\Delta C_r = \frac{2\sigma_{SL}V_S(1 - C_L)C_L}{rRT_M(C_S - C_L)} \quad (16)$$

where R is the gas constant, T_M is the melting temperature, C_S and C_L are the compositions of the equilibrated solid and liquid phases and V_S is the molar volume of the solid phase. For small changes

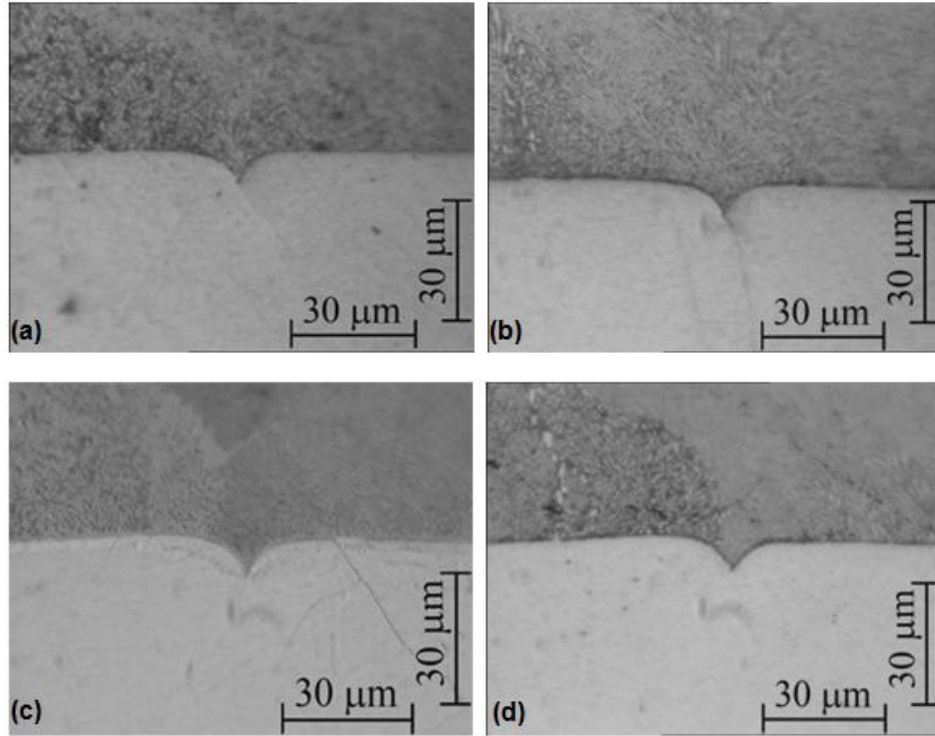


Figure 7. Typical grain boundary groove shapes for the solid Cd phase in equilibrium with the eutectic liquid.

$$\Delta T_r = m_L \Delta C_r = \frac{2m_L \sigma_{SL} V_S (1 - C_L) C_L}{r R T_M (C_S - C_L)} \quad (17)$$

where m_L is the slope of liquidus. For a spherical solid $r_1 = r_2 = r$ and the curvature undercooling is written by

$$\Delta T_r = \frac{2\sigma_{SL}}{r \Delta S^*} \quad (18)$$

From Equations 17 and 18, the entropy change for an alloy is written as:

$$\Delta S^* = \frac{R T_M (C_S - C_L)}{m_L V_S (1 - C_L) C_L} \quad (19)$$

The molar volume, V_S is expressed as:

$$V_S = V_c N_a \frac{1}{n} \quad (20)$$

where V_c is the volume of the unit cell, N_a is the Avogadro's number and n is the number of molecules per unit cell. The values of the relevant constant used in the determination of entropy change per unit volume are given in Table 3. The entropy of fusion per unit volume for the solid Cd phase is found to be $(1.533 \pm 0.076) \times 10^6 \text{ J/K m}^3$.

The solid-liquid interface energy (σ_{SL})

The solid-liquid interface energy (σ_{SL}) can be obtained from the Gibbs-Thomson equation for isotropic interfacial energy (Gündüz and Hunt, 1985, 1989; Maraşlı and Hunt, 1996; Akbulut et al., 2009; Ocağ et al., 2010; Meydaneri et al., 2011, 2012) and it is expressed as:

$$\Gamma = \frac{\sigma_{SL}}{\Delta S^*} \quad (21)$$

The solid-liquid interface energy for the solid Cd solution in equilibrium with the eutectic liquid solution was obtained using the values of the Gibbs-Thomson coefficient and the entropy of fusion per unit volume. The value of the solid-liquid interface energy was found to be $(128.00 \pm 12.8) \times 10^{-3} \text{ Jm}^{-2}$. A comparison with previous works is also shown in Table 4. The value of σ_{SL} is in good agreement with previous theoretically and experimentally calculated values of σ_{SL} for solid Cd.

Grain boundary energy

According to force balance at the grain boundary groove, if the solid-liquid interface energy is calculated, it is possible to determine the grain boundary energy. When

Table 3. Some physical properties of solid Cd phase in the Cd-Pb alloy system.

System	For solid Cd phase in the Cd-Pb alloy
Composition of solid phase, C _s	Solid Cd (solid Cd-0.25 wt.% Pb) (Hansen and Anderko, 1985)
Composition of quenched liquid phase, C _L	Eutectic Liquid (Cd-17.4 wt.% Pb) (Hansen and Anderko, 1985)
The value of f(C) for solid Cd	-3.56 (Hansen and Anderko, 1985)
Melting Temperature, T _M (K)	521 (Hansen and Anderko, 1985)
Liquidus slope of solid Cd, m _L (K/at.fr.)	-774 (Hansen and Anderko, 1985)
Crystal structure of solid Cd	Hexagonal A3
Lattice parameters of Cd (Å)	a = 2.978, c = 5.617
n	6
Molar volume of solid Cd, V _S × 10 ⁻⁶ (m ³)	12.99
Molar mass of Cd (g)	112.40
Density (g/cm ³)	8.65
Entropy change of fusion for solid Cd, ΔS* (J/Km ³)	1.533 ± 0.076 × 10 ⁶

$$f(C) = \frac{C_s - C_L}{(1 - C_L)C_L}$$

Table 4. A comparison of the σ_{SL} , σ_{GB} and Γ values for solid Cd phase obtained in the present work with the values of σ_{SL} , σ_{GB} and Γ obtained in previous works.

System	Liquid phase (C _L)	Solid phase (C _S)	Temperature (K)	$\Gamma \times 10^{-8}$ (Km)	$\sigma_{SL} \times 10^{-3}$ (J m ⁻²)	$\sigma_{GB} \times 10^{-3}$ (J m ⁻²)
Bi-Cd (Keşlioğlu et al., 2004)	Cd-0.03 at.% Bi	Bi-54.6 at.% Cd	418.7	8.28 ± 0.33	81.22 ± 7.31	154.32 ± 18.52
Cd-Zn (Saatçi and Pamuk, 2006)	Cd-5.0 at.% Zn	Cd-26.5 at. % Zn	539	8.16 ± 0.65	121.46 ± 0.97	242.38 ± 1.93
Cd-Pb [PW]	Cd-17.4 wt.% Pb	Cd-0.25 wt. % Pb	521	8.35 ± 0.41	128.00 ± 12.8	239.33 ± 26.32

[PW]: Present work.

the interface energy is isotropic, the force balance can be expressed as:

$$\sigma_{SS} = \sigma_{SL}^A \cos \theta_A + \sigma_{SL}^B \cos \theta_B \quad (22)$$

where θ_A and θ_B are the angles that the solid-liquid interfaces make with the y- axis. If the grains on either side of the grain boundary are approximately the same, the grain boundary energy can be expressed by:

$$\sigma_{GB} = 2\sigma_{SL} \cos \theta \quad (23)$$

where $\theta = \frac{\theta_A + \theta_B}{2}$ is the average angle value that the solid-liquid interfaces make with the y-axis. As shown in Equation 23, σ_{GB} is not sensitive to the error in θ for small θ values. According to Equation 23, the value of σ_{GB} should be smaller or equal to twice that of the solid-liquid interface energy, that is, $\sigma_{GB} \leq 2\sigma_{SL}$.

The grain boundary energy was calculated from Equation 23 using the related σ_{SL} and θ for groove

shapes. The average grain boundary energy value for the ten grain boundary groove shapes was found to be $\sigma_{GB} = (239.33 \pm 26.32) \times 10^{-3} \text{ J m}^{-2}$.

A comparison of the values of the solid Cd solution obtained in the present work with the values determined in previous works is given in Table 4.

Interfacial free energy and its anisotropy are considered to play a critical role in many phase transformations. The determination of the effects of anisotropy on the interfacial energy is very difficult. In the present work, the interfacial energy of the solid Cd solution in equilibrium with the eutectic liquid solution was assumed to be isotropic.

The experimental error ratio in the present work

The coordinates of the equilibrated grain boundary groove shapes were measured with an optical microscope to an accuracy of $\pm 10 \mu\text{m}$.

The thickness of the sample for geometrical correction was measured with a digital micrometer with $\pm 1 \mu\text{m}$ resolution. Thus, the error ratio in the measurements of

the equilibrated grain boundary coordinates was less than 0.2%.

The experimental error ratio in the measurement of κ_S is the sum of the fractional uncertainty of the measurements of power, temperature differences, length of heating wire and position of thermocouples which can be expressed as:

$$\left| \frac{\Delta \kappa_S}{\kappa_S} \right| = \left| \frac{\Delta Q}{Q} \right| + \left| \frac{\Delta T_1}{T_1} \right| + \left| \frac{\Delta T_2}{T_2} \right| + \left| \frac{\Delta \ell}{\ell} \right| + \left| \frac{\Delta r_1}{r_1} \right| + \left| \frac{\Delta r_2}{r_2} \right| \quad (24)$$

The experimental error ratio in the thermal conductivity measurements is found to be about 5%.

The experimental error ratio in the measurement of the temperature gradient of the solid phase is the sum of the fractional uncertainty of the power measurement, length of heating wire, thermal conductivity and thermocouples' positions which can be expressed as:

$$\left| \frac{\Delta G_S}{G_S} \right| = \left| \frac{\Delta Q}{Q} \right| + \left| \frac{\Delta \ell}{\ell} \right| + \left| \frac{\Delta r}{r} \right| + \left| \frac{\Delta \kappa_S}{\kappa_S} \right| \quad (25)$$

If Equation 25 is compared with Equation 24, the experimental errors from the measurements of Q , ℓ , r , ΔT in Equation 25 already exist in the fractional uncertainties at Equation 24. Thus, the total experimental error in the temperature gradient measurements is equal to the experimental error in the thermal conductivity measurements and is about 5%.

The experimental error ratio in the determination of the Gibbs-Thomson coefficient is the sum of the experimental error ratios in the measurements of the temperature gradient, thermal conductivity and groove coordinates. Thus, the total error ratio in the determination of the Gibbs-Thomson coefficient is about 5%. The error ratio in the determined entropy change of fusion per unit volume is estimated to be about 5% (Tassa and Hunt, 1976).

The experimental error ratio in the determination of solid-liquid interfacial energy is the sum of the experimental error ratios of the Gibbs-Thomson coefficient and the entropy change of fusion per unit volume. Thus, the total experimental error ratio of the solid-liquid interfacial energy obtained in the present work is about 10%. The experimental error ratio in the determination of θ angles was found to be 1%. Thus, the total experimental error ratio in the resulting grain boundary energy is about 11%.

Conclusion

(1) The equilibrated grain boundary groove shapes were obtained for the solid Cd solution in equilibrium with the eutectic liquid by using a radial heat flow apparatus, and the Gibbs-Thomson coefficient, Γ , was calculated to be $\Gamma = (8.35 \pm 0.41) \times 10^{-8}$ Km by using the groove shapes.

(2) The effective entropy change per unit volume, ΔS^* , was calculated to be $(1.533 \pm 0.076) \times 10^6$ J/Km³ by using the phase diagrams and related parameters.

(3) The solid-liquid interface energy, σ_{SL} , was determined to be $\sigma_{SL} = (128.00 \pm 12.8) \times 10^{-3}$ Jm⁻² from the Gibbs-Thomson equation by using the Gibbs-Thomson coefficient, Γ , and the effective entropy change, ΔS^* .

(4) The grain boundary energy, σ_{GB} , was determined to be $\sigma_{GB} = (239.33 \pm 26.32) \times 10^{-3}$ Jm⁻² by using the angle θ and the related σ_{SL} .

ACKNOWLEDGEMENTS

This work was financially supported by the Erciyes University Research Foundation under Contract No: FBD-09-846. The authors are grateful to the foundation for its financial support.

REFERENCES

- Akbulut S, Ocak Y, Maraşlı N, Keşlioğlu K, Kaya H, Çadırlı E (2009). Determination of interfacial energies of solid Sn solution in the In-Bi-Sn ternary alloy. *Mater. Charact.* 60:183-192.
- Aksöz S, Ocak Y, Maraşlı N, Keşlioğlu K (2011). Determination of thermal conductivity and interfacial energy of solid Zn solution in the Zn-Al-Bi eutectic system. *Exp. Therm Fluid Sci.* 35:395-404.
- Bulla A, Carreno-Bodensiek C, Pustal B, Berger R, Bührig-Polaczek A, Ludwig A (2007). Determination of the solid-liquid interface energy in the Al-Cu-Ag system. *Metall. Mater. Trans. A* 38:1956-1964.
- Christian JW (1975). *The theory of transformations in metals and alloys*. part I, 2nd ed., Oxford, Pergamon, P. 169.
- Erol M, Keşlioğlu K, Şahingöz R, Maraşlı N (2005). Experimental determination of thermal conductivity of solid and liquid phases in Bi-Sn and Zn-Mg binary eutectic alloys. *Met. Mater. Int.* 11:421-428.
- Gündüz M, Hunt JD (1985). The measurement of solid-liquid surface energies in the Al-Cu, Al-Si and Pb-Sn systems. *Acta. Metall.* 33:1651-1672.
- Gündüz M, Hunt JD (1989). Solid-liquid surface-energy in the Al-Mg system. *Acta. Metall.* 37:1839-1845.
- Hansen M, Anderko K (1985). *Constitutions of binary alloys*. 2nd ed, New York: McGraw-Hill. P. 432.
- Keşlioğlu K, Erol M, Maraşlı N, Gündüz M (2004). Experimental determination of solid-liquid interfacial energy for Cd in Bi-Cd liquid solutions. *J. Alloy. Compd.* 385:207-213.
- Maraşlı N, Hunt JD (1996). Solid-liquid surface energies in the Al-CuAl₂, Al-NiAl₃ and Al-Ti systems. *Acta. Mater.* 44:1085-1096.
- McCartney DG (1981). D.Phil. Thesis. University of Oxford, UK, pp. 85-175.
- Meydaneri F, Payveren M, Saatçi B, Özdemir M, Maraşlı N (2012). Experimental determination of interfacial energy for solid Zn solution in the Sn-Zn eutectic system. *Met. Mater. Int.* 18:95-104.
- Meydaneri F, Saatçi B, Özdemir M (2011). Experimental determination of solid-liquid interfacial energy for solid Sn in the Sn-Mg system. *Appl. Surf. Sci.* 257:6518-6526.
- Ocak Y, Akbulut S, Maraşlı N, Keşlioğlu K (2010). Interfacial energies of solid Sn solution in the Sn-Ag-In ternary alloy. *Chem. Phys. Lett.* 496:263-269.
- Ocak Y, Aksöz S, Maraşlı N, Keşlioğlu K (2010). Experimental determination of thermal conductivity and solid-liquid interfacial energy of solid Ag₃Sn in the Ag-Sn-In ternary alloy. *Intermetallic* 18:2250-2258.

- Porter DA, Easterling KE (1991). Phase transformations in metals and alloys. Van Nostrand Reinhold Co. Ltd. UK, P. 204.
- Saatçi B, Çimen S, Pamuk H, Gündüz M (2007). The interfacial free energy of solid Sn on the boundary interface with liquid Cd-Sn eutectic solution. *J. Phys. Condens. Matter.* 19:326219-326230.
- Saatçi B, Pamuk H (2006). Experimental determination of solid-liquid surface energy for Cd solid solution in Cd-Zn liquid solutions. *J. Phys: Condens. Mater.* 18:10143-10155.
- Tassa M, Hunt JD (1976). The measurement of Al-Cu dendrite tip and eutectic interface temperatures and their use for predicting the extent of the eutectic range. *J. Cryst. Growth* 34:38-48.
- Touloukian YS, Powell RW, Ho CY, Klemens PG (1970). Thermal conductivity metallic elements and alloys. New York: Plenum 1:48, 187.
- Woodruff DP (1973). *The Solid-Liquid Interface.* vol. 36, Cambridge University Press, Cambridge, pp. 1-2.